Fish & Shellfish Immunology 57 (2016) 186–197

Contents lists available at ScienceDirect

Fish & Shellfish Immunology

journal homepage: www.elsevier.com/locate/fsi

Full length article

Characterization of a 1-cysteine peroxiredoxin from big-belly seahorse (*Hippocampus abdominalis*); insights into host antioxidant defense, molecular profiling and its expressional response to septic conditions

G.I. Godahewa [a, b, 1], N.C.N. Perera [a, b, 1], Don Anushka Sandaruwan Elvitigala [a, b, c], R.G.P.T. Jayasooriya [a], Gi-Young Kim [a], Jehee Lee [a, b, *]

[a] Department of Marine Life Sciences, Jeju National University, Jeju Self-Governing Province, 63243, Republic of Korea
[b] Fish Vaccine Research Center, Jeju National University, Jeju Self-Governing Province, 63243, Republic of Korea
[c] Department of Zoology, University of Sri Jayewardenepura, Gangodawila, Nugegoda, 10250, Sri Lanka

ARTICLE INFO

Article history:
Received 11 May 2016
Received in revised form
6 August 2016
Accepted 13 August 2016
Available online 16 August 2016

Keywords:
Big belly seahorse
Peroxiredoxin 6
H_2O_2 scavenging
Immune stimulation
Transcriptional responses

ABSTRACT

1-cysteine peroxiredoxin (Prx6) is an antioxidant enzyme that protects cells by detoxifying multiple peroxide species. This study aimed to describe molecular features, functional assessments and potential immune responses of Prx6 identified from the big-belly seahorse, *Hippocampus abdominalis* (HaPrx6). The complete ORF (666 bp) of *HaPrx6* encodes a polypeptide (24 kDa) of 222 amino acids, and harbors a prominent peroxiredoxin super-family domain, a peroxidatic catalytic center, and a peroxidatic cysteine. The deduced amino acid sequence of HaPrx6 shares a relatively high amino acid sequence similarity and close evolutionary relationship with *Oplegnathus fasciatus* Prx6. The purified recombinant HaPrx6 protein (rHaPrx6) was shown to protect plasmid DNA in the Metal Catalyzed Oxidation (MCO) assay and, together with 1,4-Dithiothreitol (DTT), protected human leukemia THP-1 cells from extracellular H_2O_2-mediated cell death. In addition, quantitative real-time PCR revealed that *HaPrx6* mRNA was constitutively expressed in 14 different tissues, with the highest expression observed in liver tissue. Inductive transcriptional responses were observed in liver and kidney tissues of fish after treating them with bacterial stimuli, including LPS, *Edwardsiella tarda*, and *Streptococcus iniae*. These results suggest that HaPrx6 may play an important role in the immune response of the big-belly seahorse against microbial infection. Collectively, these findings provide structural and functional insights into *HaPrx6*.

1. Introduction

Species of fish and shellfish are challenged by a variety of pathogenic organisms and hazardous substances in marine aquatic ecosystems. They are vulnerable to different oxidative stresses, which can be caused by i) biological components, such as pathogenic microorganisms and toxic algae; ii) physical components, such as UV radiation and high temperature; and iii) chemical factors, including heavy metal pollutants [1]. Reactive oxygen species (ROS) encompass a number of reactive molecules that are naturally produced as byproducts of aerobic metabolism in somatic cells [2], including superoxide anions ($O_2^{\bullet-}$), superoxide radicals (O_2^-), singlet oxygen ($^1O_2$), hydrogen peroxide (H_2O_2), and hydroxyl radicals ($OH^\bullet$) [3]. These ROS are vital for various cellular functions, like cell proliferation, cell differentiation, maintaining intracellular signaling cascades [4–6], and eliciting immune responses [7,8]. However, excessive levels of free radicals may cause serious damage to host cells, including DNA strand breaks, lipid peroxidation, protein oxidation, and cell death [9]. To protect host cells from oxidative stress, aerobic cells have developed a potent antioxidant defense system comprised of molecular antioxidants, such as catalase (CAT), superoxide dismutase (SOD), glutathione peroxidase (Gpx), and peroxiredoxin (Prx) enzymes.

Thiol-specific antioxidant enzymes of the Prx family can prevent cellular oxidative damage [10]. Those Prx family members contain the catalytically active cysteine (Cys) residues at N- or C-terminals, even though the N-terminal region is directly involved in peroxidase activity [11]. Based on the number of catalytically active Cys

* Corresponding author. Marine Molecular Genetics Lab, Department of Marine Life Sciences, College of Ocean Science, Jeju National University, 66 Jejudaehakno, Ara-Dong, Jeju Self-Governing Province, 63243, Republic of Korea.
E-mail address: jehee@jejunu.ac.kr (J. Lee).
[1] These authors contributed equally to this work.

http://dx.doi.org/10.1016/j.fsi.2016.08.028
1050-4648/

residues, Prxs are categorized into three main subgroups: typical 2-Cys Prxs (Prx1, Prx2, Prx3, Prx4), atypical 2-Cys Prx (Prx5), and 1-Cys Prx (Prx6). Among the six Prx subgroups, Prx 6 consists of a single catalytically active peroxidatic Cys, while the others contain two redox-active Cys residues [12]. Peroxiredoxins are crucial for the reduction of hydrogen peroxide, peroxynitrite, and organic hydroperoxides (ROOH) through their peroxidase activity ($ROOH + 2e^- \rightarrow ROH + H_2O$) [13,14]. In addition, Prxs are associated with host immune responses against viral and bacterial infections [12,15].

Prx6 is referred to as a "bifunctional" enzyme; it is a crucial participant in cellular redox reactions that protect cells against oxidative injury [12], and is also involved in phospholipid metabolism *via* its Ca^{2+}-independent phospholipase A_2 activity [16–18]. Prx6s are restricted to the cytosol, which enables them to function efficiently [19], however, the catalytic efficacies of the Prx family are comparatively lower than those of CAT or Gpx [20]. To date, several reports have described the functional and transcriptional responses of Prx6 derived from the kingdoms, Animalia and Plantae. However, comprehensive studies exploring structure and function at the sequence level or host immune responses elicited by Prx6 are limited to only a few fish species. Hence, further studies in other teleost species, like the big-belly seahorse, would broaden the understanding of Prx6 and its associated functions.

The big-belly seahorse (*Hippocampus abdominalis*) is an important aquaculture species that has been used as a traditional medicine in Asian countries like Korea, China, and Japan. Due to overexploitation and pathogenic attacks [21,22], the seahorse is categorized under appendix II of CITES (the Convention on International Trade in Endangered Species of Wild Fauna and Flora). In addition, unfavorable environmental stress conditions lead to the suppression of immunity in aquatic animals, but an understanding of stress responses and immune mechanisms in the seahorse is currently lacking. Therefore, to broaden our understanding of the physiology and immunity of seahorses, the present study focused on the characterization of big-belly seahorse peroxiredoxin 6 (*HaPrx6*) in terms of its molecular sequence features and structure, the antioxidant activity of its recombinant protein, tissue-specific mRNA expression, and mRNA expression in response to bacterial challenges.

2. Methodology

2.1. H. abdominalis transcriptomic database construction

A seahorse transcriptomic database was constructed by the 454 GS-FLX™ sequencing technique. Briefly, total RNA from blood, liver, kidney, gill, and spleen tissues of 18 seahorses was extracted and purified with an RNeasy Mini kit (Qiagen, USA), followed by assessment of quality and quantity using an Agilent 2100 Bioanalyzer (Agilent Technologies, Canada). In order to prepare the GS-FLX 454 shotgun database, RNA was fragmented into an average size of 1147 bp using the Titanium system (Roche 454 Life Science, USA). Sequencing was performed on half of a picotiter plate on a Roche 454 GS-FLX™ DNA platform by Macrogen Corp (Korea). The raw 454 reads were trimmed to remove adaptor and low-quality sequences, and *de novo* assembled into contigs using GS Assembler (Roche 454 Life Science, USA) with default parameters set.

2.2. HaPrx6 cDNA sequence identification

A putative *HaPrx6* cDNA contig (Accession number: KX228392) that showed homology with known Prx6 counterparts was identified and isolated from the seahorse transcriptomic database. The *HaPrx6* sequence was affirmed through homology screening by the BLAST algorithm (http://blast.ncbi.nlm.nih.gov/Blast.cgi), available from the National Center for Biotechnology Information (NCBI).

2.3. Bioinformatics profiling

HaPrx6 cDNA was subjected to DNAssist version 2.2 to obtain the putative coding sequence (CDS) and to derive the corresponding protein sequence. The functional domain search was accomplished using the conserved domain search program (CDD; http://www.ncbi.nlm.nih.gov/cdd) at NCBI. Conserved cysteine residues were predicted using the Cys finder (http://clavius.bc.edu/~clotelab/DiANNA/). Potential *N*-linked glycosylation sites were predicted *via* the NetNGlyc web server (http://www.cbs.dtu.dk/services/NetNGlyc/). Pairwise amino acid identity and similarity between homologues were evaluated by the MatGAT program [23]. Multiple sequence alignment was performed using the ClustalW2 program (http://www.ebi.ac.uk/Tools/msa/clustalw2/). The phylogenetic tree was constructed using the neighbor-joining (NJ) method available in the Molecular Evolutionary Genetics Analysis (MEGA v 5.0) program [24], with bootstrap values calculated for 5000 replications to estimate the robustness of internal branches. The folding pattern for the tertiary arrangement of the HaPrx6 protein sequence was predicted using the FoldIndex© (http://bip.weizmann.ac.il/fldbin/findex) online bioinformatics tool [25].

2.4. Cloning of HaPrx6 CDS

The cDNA fragment encoding the CDS of the *HaPrx6* gene was cloned into the pMAL-c5X vector (New England Biolabs, USA) after carrying out a restriction digestion at *Nde* I and *Bam*H I sites (Supplementary Table 1) using corresponding enzymes. Briefly, PCR was performed for a 50 μL reaction containing 50 ng of liver cDNA, 5 μL of 10 × *Ex Taq* Buffer, 4 μL of 2.5 mM dNTPs, 25 pmol of each primer, and 5 units (U) of *Ex Taq* polymerase (TaKaRa, Japan). The PCR cyclic conditions were as follows: an initial denaturation at 95 °C for 5 min, 30 cycles of amplification at 95 °C for 30 s, 58 °C for 30 s, and 72 °C for 1 min, followed by a final extension at 72 °C for 5 min. The restriction digested *HaPrx6* cDNA fragment and the pMAL-c5X vector were gel purified using an Accuprep™ gel purification kit (Bioneer, Korea). Overnight ligation was then continued at 4 °C using the Mighty Mix DNA Ligation Kit (TaKaRa, Japan). Subsequently, the recombinant construct was transformed into *Escherichia coli* DH5α competent cells, and positive clones were confirmed by restriction digestion followed by sequence verification (Macrogen, Korea). Finally, the sequence verified recombinant construct was transformed into *E. coli* ER2523 (New England BioLabs, UK) competent cells for protein expression.

2.5. Overexpression and purification of recombinant HaPrx6 (rHaPrx6)

rHaPrx6 fusion protein expression and purification were carried out as described in our previous study [12], following the instructions for the pMAL Protein Fusion and Purification System (New England Biolabs, USA). Recombinant maltose binding protein (rMBP) was also expressed and purified under the same conditions. rHaPrx6 and rMBP protein concentrations were determined by the Bradford assay [26]. Purified protein samples were further analyzed on a 12% SDS-PAGE gel along with a protein marker (Enzynomics, Korea) in order to examine the degree of rHaPrx6 protein induction, purity, and integrity. The SDS-PAGE gel was stained with 0.05% Coomassie blue R-250 and subjected to a standard de-staining procedure.

2.6. Metal-catalyzed oxidation (MCO) assay

The MCO assay was conducted to assess the DNA protection

activity of rHaPrx6 as described earlier by De Zoysa et al. [27], with slight modifications. In brief, a total volume of 100 μL of a reaction mixture containing the MCO system (4 mM dithiothreitol, DTT; 30 μM $FeCl_3$; and H_2O) and different concentrations of purified rHaPrx6 (6.25–100 μg/mL) was incubated for 2 h at 37 °C. Afterwards, 1000 ng of pUC19 DNA was added to each reaction mixture, and incubated for 2.5 h at 37 °C. Purified rMBP- and bovine serum albumin (BSA)-treated samples were used as controls. Finally, reaction mixtures were terminated *via* PCR purification using a commercial PCR products purification kit (Bioneer, Korea) according to the vendor's protocol, and then samples were analyzed on a 1% agarose gel stained with ethidium bromide.

2.7. Effect of rHaPrx6 on cell protection during oxidative stress

In order to determine whether rHaPrx6 can protect human leukemia THP-1 cells from oxidative stress mounted by H_2O_2, we conducted the cell viability 3-(4,5-dimethylthiazol-2-yl)-2,5-diphenyl tetrazolium bromide (MTT) assay as described in Refs. [12,28], with slight modifications. Briefly, THP-1 cells were cultured in RPMI 1640 culture medium supplemented with 10% FBS, 100 U/mL penicillin, and 100 mg/mL streptomycin in a 5% CO_2 humidified incubator at 37 °C. A set of wells containing 1×10^5 cells/mL was incubated with different concentrations of rHaPrx6 (25–100 μg/mL) or 100 μg/mL rMBP for 30 min in the presence of 1 mM DTT. Then, samples were subjected to oxidative stress by 400 μmol H_2O_2 for 24 h. Subsequently, the viability of THP-1 cells was detected by the standard MTT assay.

2.8. Detection of apoptosis

Flow cytometry was conducted to detect the percentage of viable versus apoptotic cells in THP-1 cell populations after H_2O_2 oxidative stress as described in Ref. [12], with slight modifications. Briefly, THP-1 cells were cultured as described in section 2.7 and cells were incubated with different concentrations of rHaPrx6 (25–100 μg/mL) or 100 μg/mL rMBP for 30 min in the presence of 1 mM of DTT. Then, samples were exposed to oxidative stress by 400 μmol H_2O_2 for 24 h and then washed with PBS. Finally, cells were stained with annexin-V (ApopNexin Annexin-V FITC Apoptosis Kit) for 30 min according to the manufacturer's protocol (EMD Millipore, USA). Stained apoptotic cells were then analyzed on a BD FACScalibur flow cytometer (BD Biosciences, USA) and data were analyzed using CellQuest™ Pro software (BD Biosciences). All of the experiments were performed in triplicate.

2.9. Animal husbandry and tissue sampling

Healthy seahorses (~8 g) were acquired from the Korea Marine Ornamental Fish Breeding Center on Jeju Island, and were acclimated in laboratory aquarium tanks at 20 °C for one week prior to experimentation. Six seahorses (3 male and 3 female) were aseptically dissected for tissue specific mRNA expression analysis. Blood was collected by injuring the tails, and the peripheral blood cells were separated by immediate centrifugation at 3000*g* for 10 min at 4 °C. Other tissues, including liver, intestine, kidney, pouch, ovary, gill, heart, spleen, brain, stomach, muscle, testis, and skin were excised and immediately snap frozen in liquid nitrogen and stored at −80 °C.

2.10. Immune responsive stimulation

Healthy seahorses (~3 g) were acquired from the Korea Marine Ornamental Fish Breeding Center on Jeju Island and were acclimated as described in section 2.9. To study the immune related transcriptional response of *HaPrx6* in liver and kidney tissues, fish were divided into four groups and challenged with various substances: phosphate-buffered saline (PBS), lipopolysaccharide (LPS), *Edwardsiella tarda*, and *Streptococcus iniae*, as shown in Table 1. Five individuals were randomly collected at 0, 3, 6, 12, 24, and 48 h post infection (p.i.) as described above (section 2.9), and liver and kidney tissues were collected, snap frozen in liquid nitrogen, and stored at −80 °C.

2.11. Total RNA extraction and cDNA synthesis

Total RNA was extracted from a pool of tissue samples (n = 6 for tissue specific expression analysis; n = 5 for the immune challenge) using RNAiso plus (TaKaRa) reagent followed by clean-up with an RNeasy spin column (Qiagen). RNA concentration was determined at 260 nm in a μDrop Plate reader (Thermo Scientific), and purity was examined by 1.5% agarose gel electrophoresis. First strand cDNA was synthesized as explained in Godahewa et al. [29] in a 20 μL reaction mixture containing 2.5 μg of RNA with a PrimeScript™ II 1st strand cDNA Synthesis Kit (TaKaRa). The synthesized cDNA was diluted 40-fold in nuclease-free water and stored at −20 °C until use in quantitative real time PCR (qPCR) assays.

2.12. Quantification of HaPrx6 transcript abundance by qPCR

To study spatial expression in tissues and temporal expression during an immune challenge of *HaPrx6* in the seahorse, qPCR reactions were performed in accordance with MIQE guidelines [30]. qPCR was carried out using a Thermal Cycler Dice™ TP800 (TaKaRa) in a 10 μL reaction volume containing 3 μL of diluted cDNA template, 5 μL of 2 × TaKaRa Ex Taq™ SYBR premix, 0.4 μL of each of the forward and reverse primer (10 pmol/μL) (Supplementary Table 1), and 1.2 μL of PCR grade H_2O. The qPCR cycle profile included one cycle of 95 °C for 30 s, followed by 45 cycles of 95 °C for 5 s, 58 °C for 10 s, and 72 °C for 20 s, and a final single cycle of 95 °C for 15 s, 60 °C for 30 s, and 95 °C for 15 s. Each assay was conducted in triplicate, and data were analyzed according to the Livak method [31]. In order to confirm that the primer pair used in the reaction amplified a single product of the expected size, a dissociation curve was generated and analyzed at the end of the amplification reaction, and then samples were further assessed on a 1% agarose gel. Seahorse *40S ribosomal protein S7* (Accession number: KP780177) was used as the internal control gene. Data were calculated as the quantity of *HaPrx6* mRNA normalized to the quantity of *40S ribosomal protein S7* mRNA and expressed as the mean ± SD. Tissue-specific *HaPrx6* mRNA expression levels were calculated relative to the mRNA expression level in skin. Post infection temporal expression analysis of *HaPrx6* was further normalized to the corresponding mRNA expression levels of PBS injected controls, thus keeping the expression level of untreated/un-injected (0 h) controls as the baseline expression.

2.13. Statistical analysis

Data generated from the MTT assay, flow cytometry, and qPCR assays are presented as the mean ± SD from triplicate experiments. Statistical analyses were performed with GraphPad (GraphPad Software, Inc., USA), using the unpaired, two-tailed *t*-test to calculate *P*-values. *P*-values less than 0.05 were considered statistically significant.

3. Results and discussion

3.1. Identification of HaPrx6 and in silico characterization

3.1.1. Sequence features

The Prx6 homolog of *H. abdominalis* consisted of a 1422 bp cDNA

Table 1
Summary of the immune challenges used in the current study.

Pathogen	Source	Mode	Dose/Fish	Volume
LPS	*E. coli* 055:B5, sigma	Intra-peritoneal	125 μg	100 μL
E. tarda	CNU, Korea	Intra-peritoneal	5×10^5 CFU	100 μL
S. iniae	CNU, Korea	Intra-peritoneal	1×10^7 CFU	100 μL
PBS (injection control)	–	Intra-peritoneal	–	100 μL

CNU: obtained from the Department of Aqualife Medicine at Chonnam National University (Republic of Korea).

sequence containing a 62 bp 5′ untranslated region (UTR), a 666 bp open reading frame (ORF), and a 694 bp 3′-UTR. The CDS of *HaPrx6* could be translated into a putative polypeptide of 222 amino acids. According to the DNAssist program, HaPrx6 has a predicted molecular mass of 24 kDa and a theoretical isoelectric point (*p*I) of 5.9. The CDD search results at NCBI encountered a prominent peroxiredoxin super-family domain architecture covering ~97% of the HaPrx6 amino acid sequence, which is a common feature of Prx family members. The nucleotide and deduced amino acid sequences of HaPrx6 are shown in Supplementary Fig. 1. Although several Cys residues were detected in the HaPrx6 sequence, a single peroxidase cysteine was identified in the peroxidase catalytic center (^{44}PVCTTE^{49}), which may act to cleave the peroxyl bonds of various peroxide substrates [32,33]. 2-Cys Prx members contain a resolving cysteine in order to resolve the oxidized enzyme *via* completing the catalytic cycle [34]. However, in 1-Cys Prxs, absence of the additional cysteine is compensated for by an external small-molecule or proteins that act as thiol containing electron donors [14]. Additional Cys residues in the HaPrx6 mature polypeptide can form disulfide bonds, which may be crucial for dimer formation, which is a commonly identified feature of typical 2-Cys Prx members [14]. In addition, two potential *N*-glycosylation sites (^{29}NKS^{31} and ^{191}NVS^{193}) were identified in HaPrx6, reflecting that HaPrx6 might need post-translational glycosylation modification for its biological function. Indeed, absence of a signal peptide at the N-terminal of HaPrx6 affirmed its function as an intracellular antioxidant defense mechanism. As previously reported, mammalian 1-Cys Prx is localized to the cytosol and protects tissues from reactive oxygen species during oxidative stresses [14].

3.1.2. Homology and alignment analysis

Pairwise homology comparison of HaPrx6 against other Prx6 counterparts from known vertebrates and invertebrates indicated that HaPrx6 is most closely related to the striped beakfish at 84.7% amino acid identity. In addition, fish counterparts were shown to have comparatively higher identities (>75%) with the HaPrx6 amino acid sequence, while invertebrates shared only <60% identity at the protein level (Table 2). To further validate these results, we aligned seventeen amino acid sequences of Prx6 counterparts, and found that, among them, teleostan Prx6 shared the greatest number of conserved amino acids. Furthermore, this multiple alignment analysis aided in recognizing motifs that are crucial to the structure and function of a Prx6 protein. Additionally, we noticed that higher order vertebrate species consisted of 224 amino acids, where teleost and invertebrates contained 218–223 amino acids in their protein sequences. Insertions and deletions at the amino acid level in Prx6 homologues reflect a specific molecular evolutionary pattern. As expected, the peroxidase catalytic center residues (^{44}PVCTTE^{49}) were conserved in all the assessed counterparts (Fig. 1), suggesting that they might play a crucial role in the enzymatic activity of HaPrx6 [32,33]. In addition, 1-Cys Prxs conserve a single peroxidatic cysteine, even though their amino acid sequence consists of several cysteine residues [35]. Indeed, as a characteristic feature of peroxiredoxin family, the peroxidatic cysteine of HaPrx6 (^{46}Cys) was well conserved among all the counterparts considered for the analysis [14].

Table 2
Pairwise homology comparison of the HaPrx6 amino acid sequence with Prx6 from other animal species.

Accession NO	Common name		Big-belly seahorse	Striped beakfish	Miiuy croaker	Gilt-head bream	Turbot	Atlantic cod	Rainbow trout	Atlantic salmon	Channel catfish	Zebrafish	Rock dove	Pig	Chicken	African clawed frog	Cattle	Human	House mouse	Disk abalone
			Identity %																	
	Big-belly seahorse	Similarity %		84.7	83.8	83.8	82.4	82.4	81.2	80.7	79.5	76.7	72.0	72.0	71.6	71.1	71.1	70.2	69.3	59.6
ADJ21808	Striped beakfish		92.3		92.8	91.4	92.8	88.7	86.9	86.5	85.2	82.4	78.1	75.0	77.7	75.0	74.6	74.1	73.7	62.6
AGK83638	Miiuy croaker		91.4	97.7		90.5	91.4	86.9	89.2	88.7	84.3	82.0	76.3	73.2	76.8	74.6	72.8	71.9	71.4	61.7
ADI78069	Gilt-head bream		91.0	96.8	96.8		87.8	86.0	86.0	85.6	83.4	81.5	77.2	74.1	77.2	74.6	73.2	73.7	72.3	62.2
ADJ57694	Turbot		91.9	97.3	95.9	94.6		89.1	87.4	86.9	83.9	81.1	76.8	75.0	76.3	74.6	75.0	74.6	73.7	63.1
AGK92745	Atlantic cod		91.0	93.7	93.2	91.4	95.5		86.0	85.6	83.4	79.7	76.3	74.1	74.6	73.7	74.1	73.2	73.2	63.1
NP_001158604	Rainbow trout		90.5	94.1	93.2	93.2	94.1	92.3		98.2	85.2	82.4	75.9	72.3	75.9	75.0	71.9	71.9	71.4	62.3
ACI67571	Atlantic salmon		90.5	94.1	93.2	93.2	94.1	92.3	99.1		84.8	81.5	75.9	72.3	75.9	75.0	71.9	71.9	71.4	61.9
NP_001187160	Channel catfish		89.7	91.9	91.9	91.0	92.8	91.5	93.3	93.3		85.2	77.2	73.7	77.7	72.8	73.2	74.1	73.7	64.6
NP_957099	Zebrafish		87.4	91.4	89.2	90.1	91.4	89.6	91.0	91.0	93.7		75.9	71.4	76.8	74.6	71.0	72.8	71.9	61.4
NP_001269769	Rock dove		80.8	86.6	85.7	85.3	85.3	84.4	85.7	85.7	85.7	85.7		86.7	93.8	79.5	86.7	86.2	84.9	64.0
NP_999573	Pig		81.7	85.3	84.4	84.4	83.9	82.6	83.9	83.9	84.4	84.4	93.3		86.2	80.9	97.3	93.3	89.7	63.1
NP_001034418	Chicken		81.3	85.3	83.9	83.9	83.9	83.0	85.3	85.3	85.3	84.8	96.9	93.8		79.5	86.7	85.8	85.8	65.8
NP_001082669	African clawed frog		82.6	85.7	84.8	84.4	86.2	84.4	86.2	86.2	83.9	85.7	87.9	87.5	86.6		79.6	80.0	77.3	61.3
NP_777068	Cattle		81.7	84.8	84.4	83.9	84.4	83.0	83.9	83.9	84.4	84.4	93.8	98.7	95.1	87.1		95.1	90.6	63.1
NP_004896	Human		80.8	83.9	83.5	83.0	84.4	82.6	83.9	83.9	85.3	85.3	92.4	97.3	93.8	87.5	98.7		89.7	60.9
AAP21829	House mouse		80.4	83.0	82.6	82.1	82.6	81.7	82.6	82.6	84.8	84.4	90.6	92.9	92.0	84.4	94.2	93.8		61.8
ABO26614	Disk abalone		75.2	75.1	74.7	76.0	76.9	76.0	76.1	76.1	78.5	77.0	75.4	75.4	77.2	75.4	76.3	75.9	74.6	

3.1.3. Evolutionary position

An un-rooted phylogenetic tree was constructed to demonstrate the molecular evolution of Prx family members using different vertebrate Prxs (Prx1-6), according to the NJ method. As a result, typical 2-Cys Prxs, atypical 2-Cys Prxs, and 1-Cys Prxs converged into three main clusters. In fact, the 1-Cys Prx main cluster clearly indicated the distinct clustering of teleosts and non-teleosts, where HaPrx6 was evolutionary relevant to the *O. fasciatus* Prx6 homolog (Fig. 2). According to the tree topology, HaPrx6 evolved from a common vertebrate ancestor ensuring conventional taxonomy. Until now, Prxs were identified and characterized from unicellular to multicellular organisms, signifying that they were conserved throughout evolution with the emergence of new isoforms [14]. Further, a similar clustering pattern was previously described for different organisms, revealing an ancient origin for the Prx family [9,12,36,37]. Collectively, our phylogenetic investigation strongly validates that HaPrx6 is indeed a homolog of known Prx6s.

3.1.4. Protein structure analysis

In order to predict the three dimensional-structure arrangement of HaPrx6, a fold index was determined and compared with that of other fish, mammal, and invertebrate counterparts. Here, average hydrophobicity and the absolute net charge of the amino acid were used to determine the foldability of given Prx6 amino

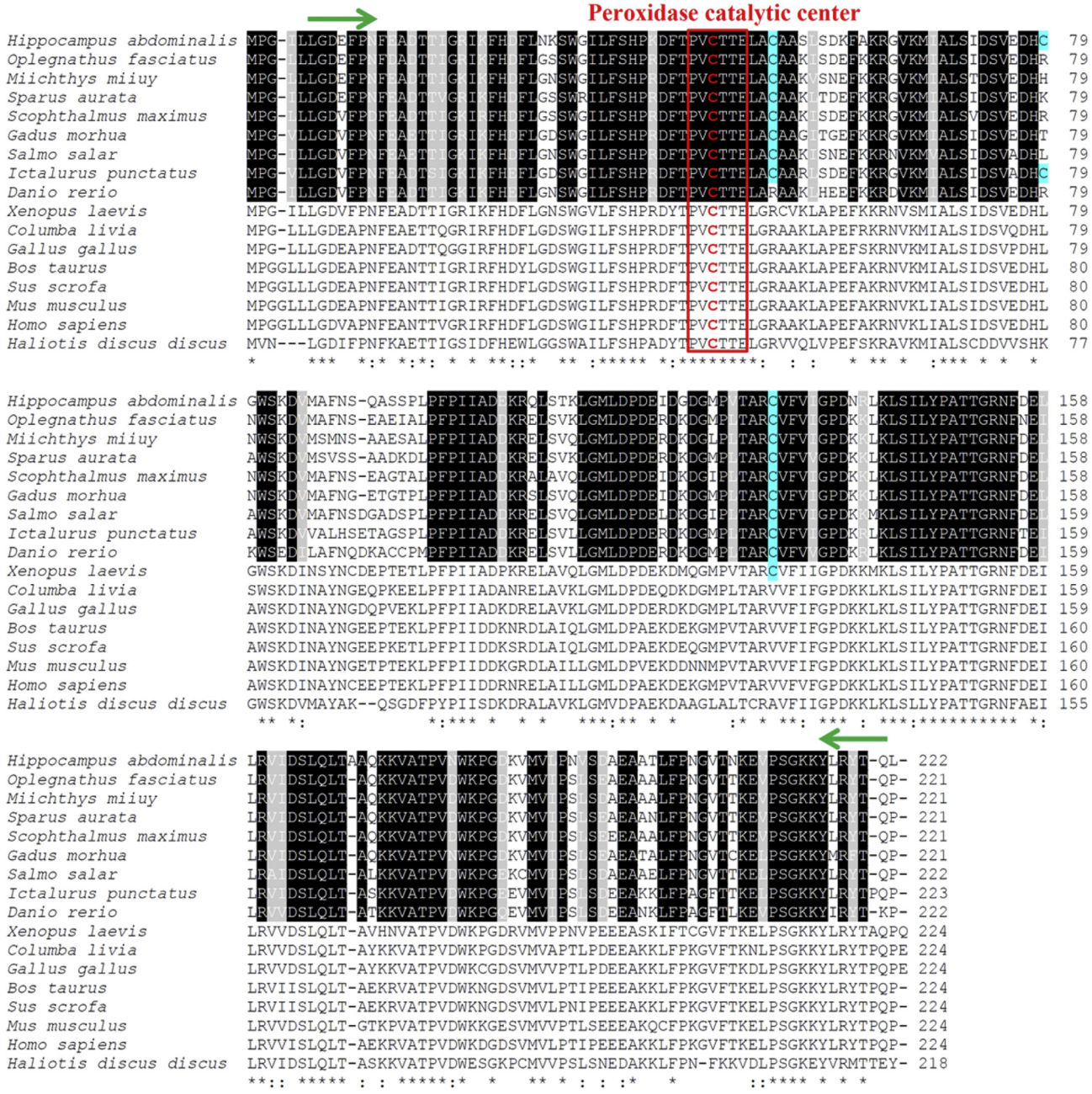

Fig. 1. Multiple sequence alignment of the HaPrx6 amino acid sequence with known Prx6 sequences. Identical residues in all sequences are indicated by (*) and conserved residues in all sequences are indicated by (:) under the column. Identical residues and conserved residues within fish counterparts are in black and gray shade, respectively. The peroxidase catalytic center is indicated by a red box. The peroxidatic cysteine residue is colored red and other cysteine residues are shaded blue. Peroxiredoxin super-family domain boundaries are denoted by green arrows. (For interpretation of the references to colour in this figure legend, the reader is referred to the web version of this article.)

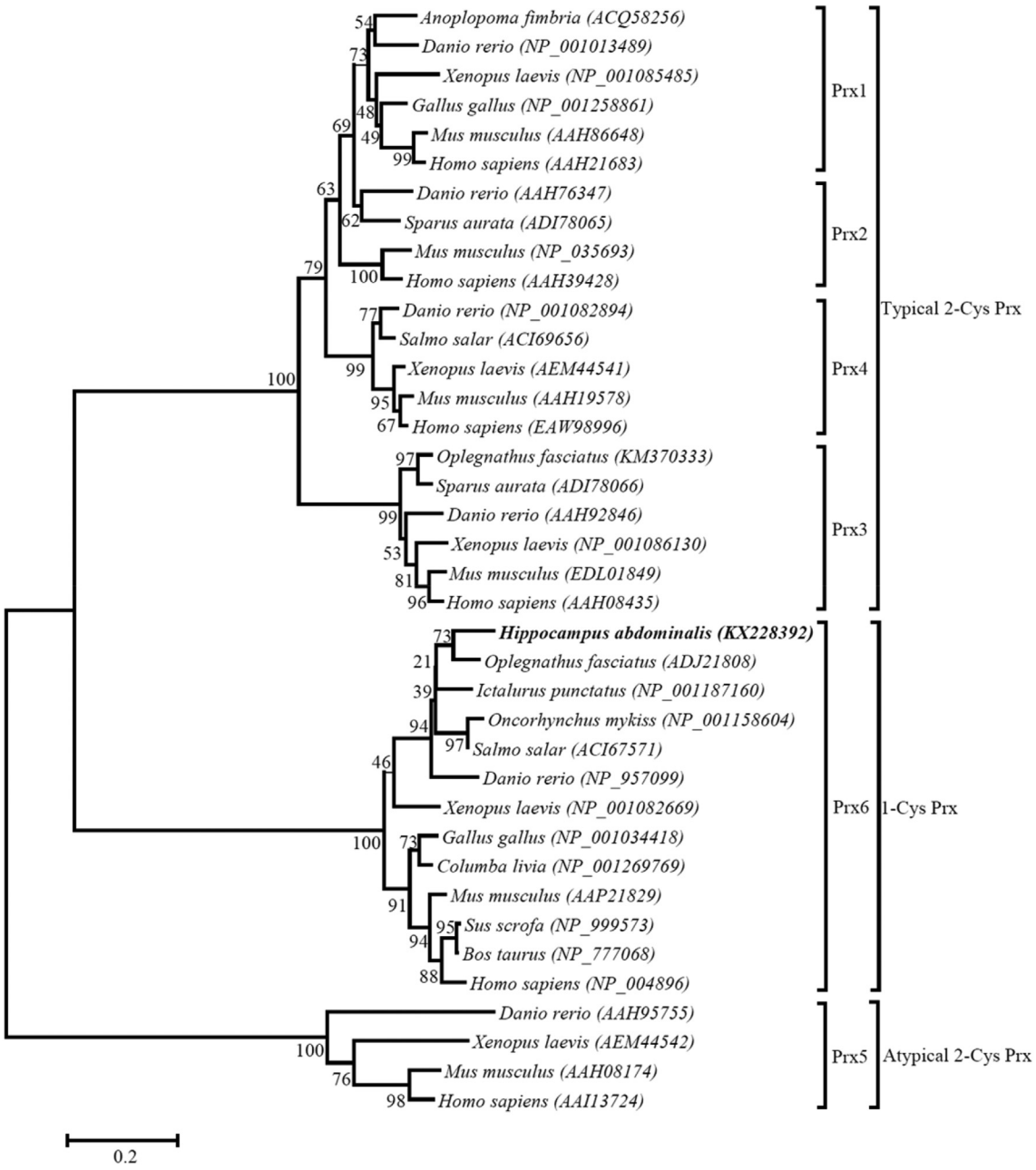

Fig. 2. Phylogenetic analysis of HaPrx6. The tree was constructed based on amino acid sequences and the number at each node indicates the percentage of bootstrapping after 5000 replications. Accession numbers are denoted next to the scientific names.

acid sequences [25]. Thus, results of the FoldIndex© tool revealed that the six Prx6 proteins analyzed were extremely folded (Fig. 3). As illustrated in Supplementary Table 2, one intrinsically unfolded/disordered region can be seen in the Prx6 sequences, with the exception of the big-belly seahorse and disk abalone. Fig. 3 shows one intrinsically unfolded/disordered region for the big-belly seahorse Prx6 sequence, which is similar to other vertebrate Prx6 counterparts. Particularly, Prx6 proteins were predicted to be well-structured, depicting their high degree of foldability, which might help them to act as an efficient antioxidant. According to a previous report, the Prxs tend to be oligomerized for redox-sensitive interactions [14]. Moreover, a folded protein can easily accomplish correct interactions with its substrates versus a disordered protein, since all the active site motifs are in the correct orientation. Moreover, the peroxiredoxin super-family domain in HaPrx6 was shown to be prominently folded, since it is enclosed within the entire amino acid sequence (Supplementary Fig. 1). Collectively, this suggests that the HaPrx6 protein is well structured and is in accordance with its biological function to acquire optimum activity. According to the present FoldIndex prediction, we can hypothesize that all the Prx6s considered herein may have an efficient antioxidant mechanism, considering the high percentage (>94%) of folded regions throughout the proteins.

3.2. Functional characterization of rHaPrx6

3.2.1. Recombinant protein overexpression and purification

The complete CDS fragment of HaPrx6 was cloned, IPTG-induced within the bacterial system, and purified by amylose affinity chromatography per the manufacturer's protocol. Induced

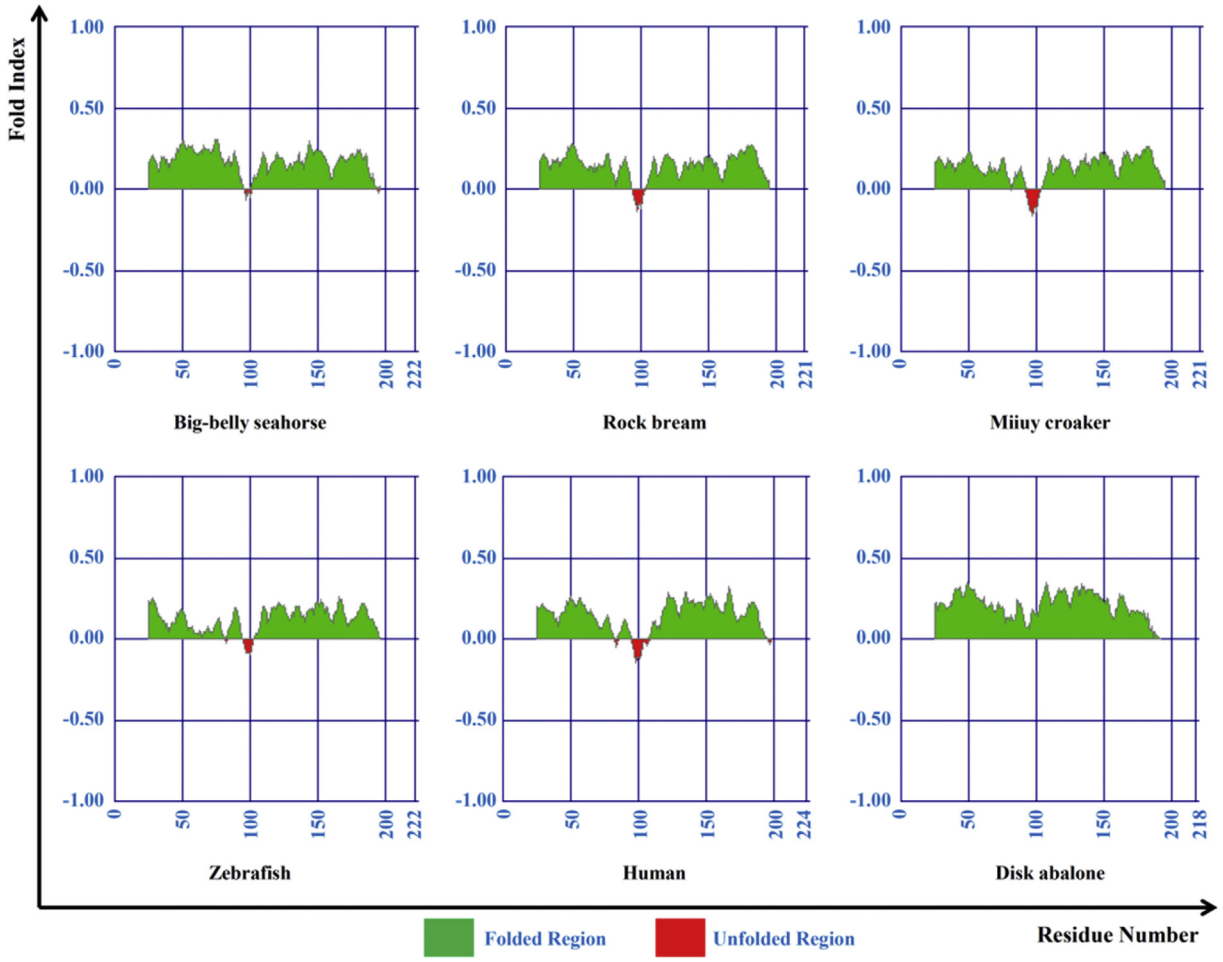

Fig. 3. Folding predictions for the tertiary structure of the HaPrx6 amino acid sequence compared to other Prx6 counterparts. Green regions indicate the folded regions, whereas unfolded regions are represented by red. (For interpretation of the references to colour in this figure legend, the reader is referred to the web version of this article.)

protein fractions were obtained at different expression and purification steps and were subjected to SDS-PAGE analysis to assess the efficacy of the whole process (Supplementary Fig. 2). Existence of bands corresponding to the rHaPrx6 fusion protein of ~66.5 kDa (HaPrx6: 24 kDa + MBP: 42.5 kDa) revealed the successful induction and purification of rHaPrx6 fusion protein in Lane I, S, and E. Afterwards, purified protein was subjected to different antioxidant assays to reveal its functional behavior as an antioxidant.

3.2.2. Metal-catalyzed oxidation (MCO) assay

The MCO system forms a platform for the auto-oxidation of DTT by varying ROS, like $O_2^{\bullet-}$, O_2^-, $^1O_2$, H_2O_2 and $OH^\bullet$. Specially, $OH^\bullet$ radicals readily react with DNA and result in DNA strand breakage. Accordingly, this ROS mediated DNA disruption results in nicked DNA due to a single strand break of supercoiled plasmid DNA [38]. Therefore, the DNA protection activity of rHaPrx6 was determined *via* the metal-catalyzed ROS generated system using the pUC19 plasmid (Fig. 4). Results showed that there is no damage to the pUC19 supercoiled DNA (B and C) when the MCO assay components are not added completely, which was indicated by the presence of the same ratio of supercoiled: nicked DNA as that of the control sample (A). However, in the presence of the complete MCO assay system, complete breakage of pUC19 DNA occurred (D and G). When 100 μg/mL BSA and rMBP was added to the MCO assay (E and F), complete breakage of supercoiled DNA into its nicked form occurred, revealing the absence of their DNA protection activity. In contrast, with increasing doses of rHaPrx6 (G: 0 μg/mL – H: 100 μg/mL), formation of nicked DNA decreased in a concentration dependent manner. Hence, the present study revealed that the MCO assay system was able to break pUC19 supercoiled DNA into its nicked form, and that this conversion can be significantly inhibited by rHaPrx6, reflecting its antioxidant activity. However, the efficacy of Prx antioxidant activity could vary depending on other factors, such as temperature, time, and pH [39]. Prxs are the most recently discovered antioxidant enzymes [14] and are active in the presence of DTT. Rock bream Prx6 [1], sheep Prx6 [40], and silkworm Prx6 [41] also demonstrated protection of supercoiled DNA in the MCO assay, and disk abalone Prx6 protected against DNA fragmentation induced by H_2O_2 [9]. In addition to Prx6, other Prx members have also been shown to protect DNA in the MCO system [42,43]. Therefore, Prxs are vital constituents of the cellular antioxidant defense system that protects live cells from ROS-mediated DNA damage.

3.2.3. Effect of rHaPrx6 on cell survival during the oxidative stress-MTT assay

Next, the extracellular H_2O_2 scavenging activity of rHaPrx6 was investigated by evaluating cell viability under oxidative stress using the MTT assay. Here, DTT acts as an electron donor to accomplish the redox reaction, where *in vivo* thioredoxin [44] or glutathione [45] would act as an electron donor. In both the *in vitro* and *in vivo* systems, this redox reaction is catalyzed by Prxs. The rHaPrx6 can react with the extracellular H_2O_2 {Prx (reduce) + H_2O_2 → Prx

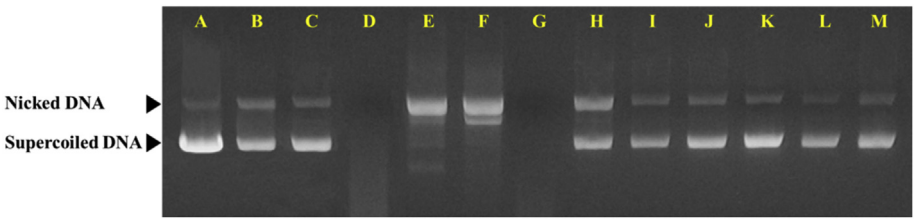

Fig. 4. Protection of supercoiled DNA cleavage by rHaPrx6 in a metal-catalyzed oxidation (MCO) system. A) pUC19 without incubation; B) pUC19 only with $FeCl_3$; C) pUC19 only with DTT; D) pUC19 with MCO system; E) pUC19 + MCO system + 100 μg/mL BSA; F) pUC19 + MCO system + 100 μg/mL rMBP; G) pUC19 + MCO system + 0 μg/mL rHaPrx6; H) pUC19 + MCO system + 6.25 μg/mL rHaPrx6; I) pUC19 + MCO system + 12.5 μg/mL rHaPrx6; J) pUC19 + MCO system + 25 μg/mL rHaPrx6; K) pUC19 + MCO system + 50 μg/mL rHaPrx6; L) pUC19 + MCO system + 75 μg/mL rHaPrx6; and M) pUC19 + MCO system + 100 μg/mL rHaPrx6.

(oxidize) + $2H_2O$} and diminish the oxidative stress of the THP-1 cells. Hence, cell viability might increase due to the antioxidant activity of the rHaPrx6. In accordance with our MTT assay, significant cell viability was noted in rHaPrx6-treated samples compared to positive controls (B) under H_2O_2 stress (Fig. 5). Because of the extracellular oxidative stress by 400 μmol H_2O_2, the mortality of THP-1 cells increased (B) compared to that of negative controls (A). However, the potential antioxidant activity of rHaPrx6 was observed in a dose-dependent manner (D-G) by the increase in cell survival, which was significantly higher than that of the recombinant MBP-treated sample (C). Specifically, 100 μg/mL of rHaPrx6 exhibited a cell survival of 38.25% compared to H_2O_2-treated samples, confirming that rHaPrx6 converts the oxidative H_2O_2 into non-oxidative H_2O. As previously reported, the H_2O_2 detoxification activity of Prx family members was assayed with supplementary thiols such as DTT [9,12,38,41,45] and they were confirmed as potent antioxidants. Also, our study illustrated that the rHaPrx6 protein protects cells against ROS-mediated oxidative stress, further corroborating that it is an active enzyme with typical antioxidant function in the big-belly seahorse.

3.2.4. *rHaPrx6 protects cell from ROS-dependent apoptosis*

To further validate the extracellular H_2O_2 scavenging activity of rHaPrx6, the extent of cell apoptosis under extracellular H_2O_2 stress was determined *via* flow cytometry. Basically, extracellular oxidative stress can increase the level of intracellular ROS, resulting in cellular apoptosis [13]. However, peroxidatic cysteine residues in Prx6 could oxidize into their sulfhydryl forms while reacting with H_2O_2 and the non-physiological electron donor, DTT [9,12]. Phosphatidylserines are common substances generated in the event of apoptosis on the cell surface, and can easily bind with annexin-V [46]. Here, we have assessed the percentage of apoptotic THP-1 cells due to H_2O_2-induced oxidative stress, and the results revealed that rHaPrx6-treated samples decreased cell apoptosis in a dose dependent manner by scavenging extracellular H_2O_2 with the help of DTT (Fig. 6). This was demonstrated by a significantly decreasing annexin-V stained cell population measured as a percentage of the total cell population. Furthermore, it affirms that the H_2O_2 scavenging activity of rHaPrx6 is thiol dependent. In the flow cytometric assay, 400 μmol of H_2O_2 was induced cell apoptosis (B) compared to negative controls (A). Also, reaction mixtures treated with rMBP showed higher cell apoptosis, similar to H_2O_2 treated samples (B), suggesting that rMBP did not have any impact on the antioxidant activity of rHaPrx6. Collectively, we can suggest that because of the rHaPrx6 antioxidant activity, extracellular oxidative stress was reduced in the rHaPrx6-treated samples and thereby cell apoptosis decreased. Similarly, disk abalone Prx6 and rock bream Prx3 demonstrated their antioxidant potential by lowering cell apoptosis [9,12]. Moreover, it was shown that human Prx5 can control DNA damage induced by H_2O_2 in mitochondria [47]. These results collectively signify the antioxidant role of rHaPrx6 *via* scavenging extracellular H_2O_2, and consequently cellular protection from apoptosis.

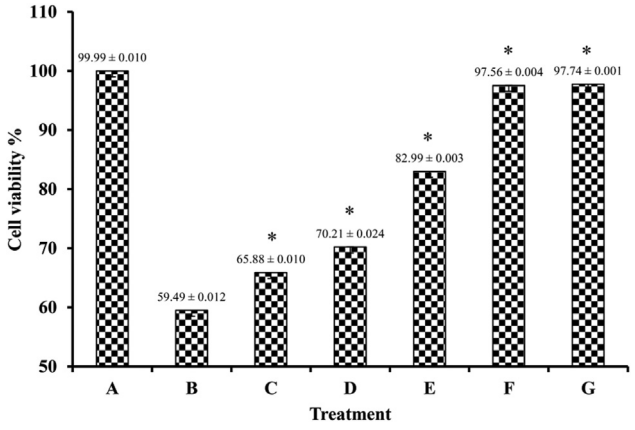

Fig. 5. Survival effect of rHaPrx6 on THP-1 cells exposed to 400 μmol of H_2O_2. A) Control cells; B) 1 mM of DTT + 400 μmol of H_2O_2; C) 100 μg/mL of rMBP with 1 mM of DTT + 400 μmol of H_2O_2; D) 25 μg/mL of rHaPrx6 with 1 mM of DTT + 400 μmol of H_2O_2; E) 50 μg/mL of HaPrx6 with 1 mM of DTT + 400 μmol of H_2O_2; F) 75 μg/mL of rHaPrx6 with 1 mM of DTT + 400 μmol of H_2O_2; and G) 100 μg/mL of rHaPrx6 with 1 mM of DTT + 400 μmol of H_2O_2. Cell survival was determined by the MTT assay in triplicate for each treatment. Vertical bars represent the cell survival % ± SD (N = 3).

3.3. *Transcriptional analysis of HaPrx6*

3.3.1. *Quantification of HaPrx6 mRNA in unchallenged tissues*

The mRNA expression profile of *HaPrx6* depicts their ubiquity in body tissues, with highest expression found in liver, followed by intestine, kidney, and pouch. Compared to these tissues, the ten other examined tissues expressed *HaPrx6* transcripts poorly (Fig. 7). *HaPrx6* expression in all tissues was compared to that in skin. Liver generates an excessive amount of ROS due to a higher metabolic rate, which may explain the pronounced *HaPrx6* mRNA expression in liver tissues observed here. Similarly, highly expressed *Prx6* in liver tissue has been documented in a few fish species, including rock bream [1], black carp [48], and gilthead sea bream [36]. In addition, disk abalone *Prx6* [9] and Chinese mitten crab *Prx6* [49] was significantly expressed in gill and hepatopancreas, respectively, while turbot *Prx6* was dominant in blood [50]. These results collectively signify that the spatial *Prx6* mRNA expression pattern is organism specific. Specifically, the present study suggests the significance of the Prx6 enzyme in several tissues as an antioxidant defense molecule. In fact, intestine is a constantly challenged organ by diet-derived toxins/oxidants and endogenously generated ROS, which can induce serious damage to cell structures [49,51]. Therefore, *HaPrx6* mRNA was significantly expressed in big-belly seahorse intestine as well. Also, immune organs like the kidney

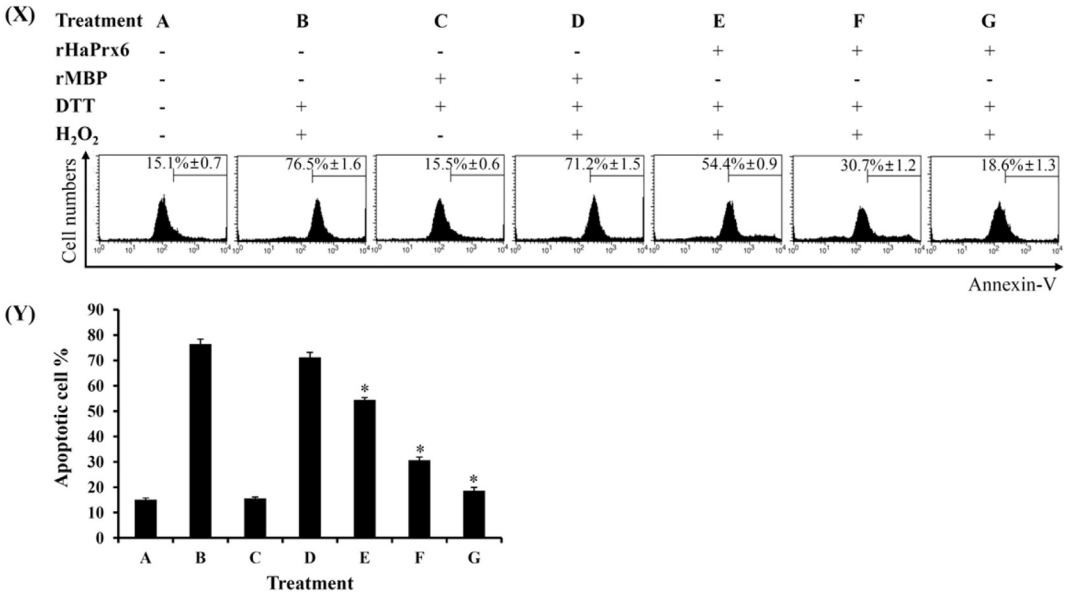

Fig. 6. Flow cytometry analysis of cell viability activity of the rHaPrx6 (X) on THP-1 cells exposed to 400 μmol of H_2O_2. A) Control cells; B) 1 mM of DTT + 400 μmol of H_2O_2; C) 100 μg/mL of rMBP with 1 mM of DTT; D) 100 μg/mL of rMBP with 1 mM of DTT + 400 μmol of H_2O_2; E) 25 μg/mL of rHaPrx6 with 1 mM of DTT + 400 μmol of H_2O_2; F) 50 μg/mL of rHaPrx6 with 1 mM of DTT + 400 μmol of H_2O_2; and G) 100 μg/mL of rHaPrx6 with 1 mM of DTT + 400 μmol of H_2O_2. Percentage of Annexin-V stained cells out of the total cell population (Y). Live and dead cells were differentiated using Annexin-V. Apoptotic cells due to intracellular ROS are expressed as gated cell percentages (N = 3; $P < 0.05$).

are likely to have strong antioxidant defense systems against ROS, which are generated as an immune response to invading microbes.

3.3.2. Quantification of HaPrx6 mRNA after bacterial stimulations

In order to explore the role of *HaPrx6* in the seahorse immune response, a time course experiment was performed after stimulation with LPS, *E. tarda*, and *S. iniae* (Fig. 8). The liver showed the greatest level of *HaPrx6* expression in healthy fish and was found to be the third-most abundant in the kidney. Since they are crucial in immune responses, liver and kidney tissues were selected for the immune responsive investigation in the present study. Though the healthy tissues were abundant in *HaPrx6* transcripts, the fold-increase was found to be less in both liver and kidney, compared to basal expression (0 h p.i.) upon the immune stimuli. However, the immune stimulation triggered significant inductive transcriptional responses of *HaPrx6* mRNA at different post-infection times in both liver and kidney tissues. Specifically, ~ 2–3 fold *HaPrx6* transcription was observed after the additional immune stimuli, suggesting its potential role in immune responses against bacterial pathogens. Upon LPS and *S. iniae* stimulation, *HaPrx6* was significantly upregulated early in both liver and kidney. However, upon *E. tarda* injection, the liver showed a late response, while the kidney showed an early response. In addition, relatively high basal expression of *HaPrx6* in liver and kidney tissues, which might be sufficient to withstand septic conditions, may explain the above observation.

It is a well-known fact that bacterial infection is a typical stress condition involving the production of ROS, which can have detrimental effects on the host [50]. On the other hand, it has been

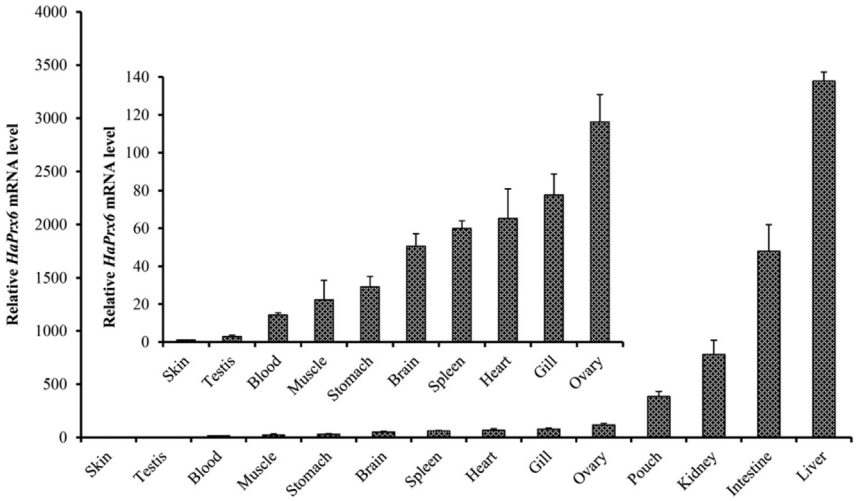

Fig. 7. Spatial analysis of *HaPrx6* mRNA expression from different big-belly seahorse tissues. *HaPrx6* tissue specific expression in skin, testis, blood, muscle, stomach, brain, spleen, heart, gill, ovary, pouch, kidney, intestine, and liver was analyzed by qPCR. mRNA expression was calculated using the Livak method relative to skin expression and normalized to 40s ribosomal protein S7 as the internal control. Data were obtained from triplicate qPCR reactions (n = 3) and presented as average values with error bars representing SD ($P < 0.05$).

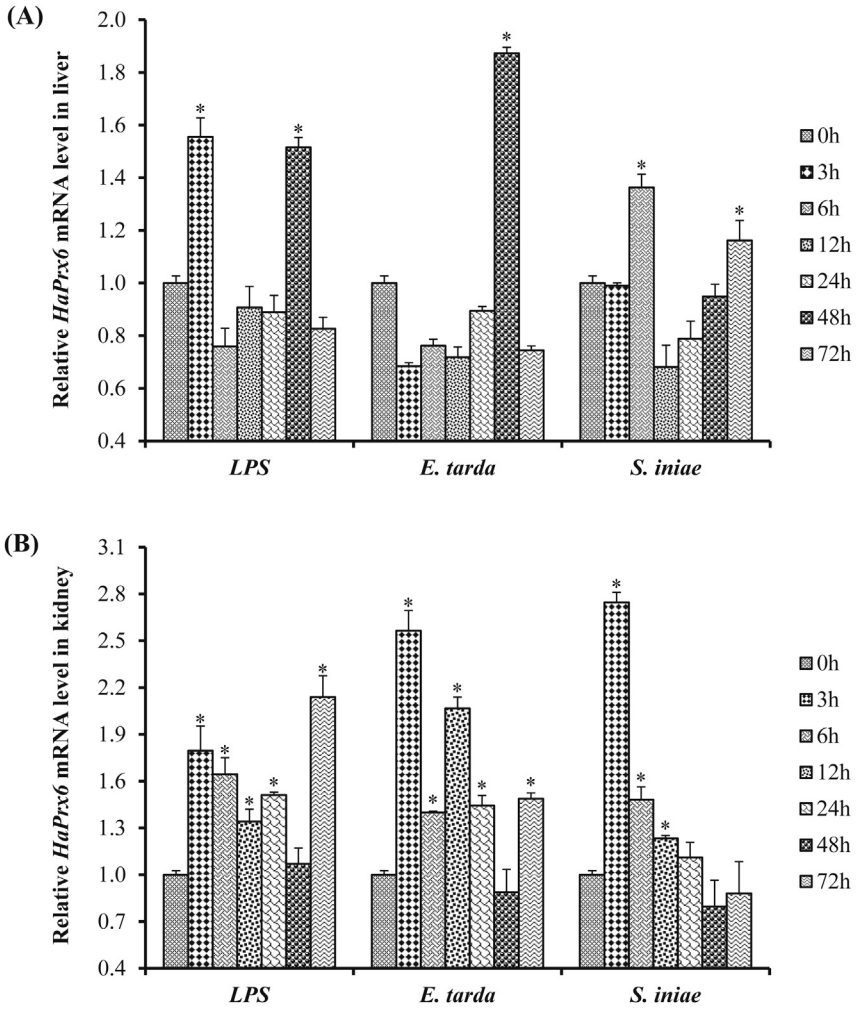

Fig. 8. *HaPrx6* mRNA expression analysis in liver (A) and kidney (B) after immune challenges. Relative mRNA expression was calculated using the Livak method relative to PBS-injected controls and normalized to 40s ribosomal protein S7 as the internal control. Data were obtained from triplicate qPCR reactions (n = 3) and presented as average values with error bars representing SD. Data shown with '*' indicates significantly different expression levels with respect to the 0 h control ($P < 0.05$).

documented that Prxs were involved in a host defense system as an antibacterial mediator [12,49,52], even though distinct antiviral responses were observed among them. Similarly, mice Prx2 has been reported to be a negative regulator of LPS-induced inflammation [15]. Together, our findings suggests that *HaPrx6* has an indispensable role in host immune responses in the big-belly seahorse, plausibly by maintaining a correct redox balance in cells, even though expression pattern and kinetics were different with regard to the immune stimuli and tissue type. Also, the observed variance in the tissue-specific *HaPrx6* induction pattern could be attributed to the difference in immune defense mechanisms that are exerted in liver and kidney tissues in the big-belly seahorse.

Even though Prxs were mainly recognized as antioxidants that combat ROS, they are known to play comprehensive roles in inflammation, transcriptional regulation, immune alterations, cell proliferation/differentiation, and apoptosis [11,13,53]. Furthermore, *Prx6* expressional upregulation at the mRNA level has been reported under stress signals, which might have functional implications in different contexts. Other homologues of *HaPrx6*, including those from the Pacific oyster, Antarctic bivalve, zebrafish, Chinese shrimp, and turbot were induced by pollution intensity [53], thermal exposure [54], brominated flame [55] and bacterial infection [50,56], respectively. Conversely, several reports have documented that Prx6 from winter flounder and disk abalone were down regulated by chromium oxide exposure [57] and viral infection [9]. Therefore, Prxs are crucial in antioxidant defense systems that can protect the host organism from ROS-mediated oxidative stress.

4. Conclusion

In conclusion, we have unequivocally identified a big-belly seahorse *Prx6* ortholog, which is similar to mammalian Prx6, with the aid of structural, functional, and transcriptional studies. HaPrx6 demonstrated specific characteristics of 1-Cys peroxiredoxins and ROS-mediated thiol-dependent antioxidant activity. In addition, investigation of transcriptional modulation revealed that *HaPrx6* mRNA expression is upregulated by bacterial infections. This might support the notion that *Prx6* could be used as an integrative biomarker of fish health and welfare, in terms of intracellular signaling and antioxidant defense. However, further studies are warranted to reveal novel functions of Prx6 in different fish species under different habitats, aquaculture systems, and infectious outbreaks.

Acknowledgement

This research was supported by the 2016 scientific promotion program funded by Jeju National University.

Appendix A. Supplementary data

Supplementary data related to this article can be found at http://dx.doi.org/10.1016/j.fsi.2016.08.028.

References

[1] M. De Zoysa, J.H. Ryu, H.C. Chung, C.H. Kim, C. Nikapitiya, C. Oh, et al., Molecular characterization, immune responses and DNA protection activity of rock bream (Oplegnathus fasciatus), peroxiredoxin 6 (Prx6), Fish Shellfish Immunol. 33 (2012) 28–35.

[2] M. Castex, P. Lemaire, N. Wabete, L. Chim, Effect of probiotic Pediococcus acidilactici on antioxidant defences and oxidative stress of Litopenaeus stylirostris under Vibrio nigripulchritudo challenge, Fish Shellfish Immunol. 28 (2010) 622–631.

[3] Y. Wang, S.I. Feinstein, Y. Manevich, Y.S. Ho, A.B. Fisher, Peroxiredoxin 6 gene-targeted mice show increased lung injury with paraquat-induced oxidative stress, Antioxid. Redox Signal 8 (2006) 229–237.

[4] B.P. Yu, Cellular defenses against damage from reactive oxygen species, Physiol. Rev. 74 (1994) 139–162.

[5] G. Ermak, K.J. Davies, Calcium and oxidative stress: from cell signaling to cell death, Mol. Immunol. 38 (2002) 713–721.

[6] J. Aguirre, M. Rios-Momberg, D. Hewitt, W. Hansberg, Reactive oxygen species and development in microbial eukaryotes, Trends Microbiol. 13 (2005) 111–118.

[7] C. Bogdan, M. Rollinghoff, A. Diefenbach, Reactive oxygen and reactive nitrogen intermediates in innate and specific immunity, Curr. Opin. Immunol. 12 (2000) 64–76.

[8] P. Roch, Defense mechanisms and disease prevention in farmed invertebrates, Aquaculture 172 (1999) 125–145.

[9] C. Nikapitiya, M. De Zoysa, I. Whang, C.G. Kim, Y.H. Lee, S.J. Kim, et al., Molecular cloning, characterization and expression analysis of peroxiredoxin 6 from disk abalone Haliotis discus discus and the antioxidant activity of its recombinant protein, Fish Shellfish Immunol. 27 (2009) 239–249.

[10] S.G. Rhee, S.W. Kang, T.S. Chang, W. Jeong, K. Kim, Peroxiredoxin, a novel family of peroxidases, IUBMB Life 52 (2001) 35–41.

[11] M.W. Robinson, A.T. Hutchinson, J.P. Dalton, S. Donnelly, Peroxiredoxin: a central player in immune modulation, Parasite Immunol. 32 (2010) 305–313.

[12] G.I. Godahewa, Y. Kim, S.H. Dananjaya, R.G. Jayasooriya, J.K. Noh, J. Lee, et al., Mitochondrial peroxiredoxin 3 (Prx3) from rock bream (Oplegnathus fasciatus): immune responses and role of recombinant Prx3 in protecting cells from hydrogen peroxide induced oxidative stress, Fish Shellfish Immunol. 43 (2015) 131–141.

[13] S.G. Rhee, H.Z. Chae, K. Kim, Peroxiredoxins: a historical overview and speculative preview of novel mechanisms and emerging concepts in cell signaling, Free Radic. Biol. Med. 38 (2005) 1543–1552.

[14] Z.A. Wood, E. Schroder, J. Robin Harris, L.B. Poole, Structure, mechanism and regulation of peroxiredoxins, Trends Biochem. Sci. 28 (2003) 32–40.

[15] C.S. Yang, D.S. Lee, C.H. Song, S.J. An, S. Li, J.M. Kim, et al., Roles of peroxiredoxin II in the regulation of proinflammatory responses to LPS and protection against endotoxin-induced lethal shock, J. Exp. Med. 204 (2007) 583–594.

[16] T.S. Kim, C.S. Sundaresh, S.I. Feinstein, C. Dodia, W.R. Skach, M.K. Jain, et al., Identification of a human cDNA clone for lysosomal type Ca2+-independent phospholipase A2 and properties of the expressed protein, J. Biol. Chem. 272 (1997) 2542–2550.

[17] Y. Manevich, A.B. Fisher, Peroxiredoxin 6, a 1-Cys peroxiredoxin, functions in antioxidant defense and lung phospholipid metabolism, Free Radic. Biol. Med. 38 (2005) 1422–1432.

[18] A.B. Fisher, Peroxiredoxin 6: a bifunctional enzyme with glutathione peroxidase and phospholipase A(2) activities, Antioxid. Redox Signal 15 (2011) 831–844.

[19] A.B. Fisher, C. Dodia, Y. Manevich, J.W. Chen, S.I. Feinstein, Phospholipid hydroperoxides are substrates for non-selenium glutathione peroxidase, J. Biol. Chem. 274 (1999) 21326–21334.

[20] H.Z. Chae, H.J. Kim, S.W. Kang, S.G. Rhee, Characterization of three isoforms of mammalian peroxiredoxin that reduce peroxides in the presence of thioredoxin, Diabetes Res. Clin. Pract. 45 (1999) 101–112.

[21] J.L. Balcazar, A. Gallo-Bueno, M. Planas, J. Pintado, Isolation of Vibrio alginolyticus and Vibrio splendidus from captive-bred seahorses with disease symptoms, Antonie Van Leeuwenhoek 97 (2010) 207–210.

[22] A.C. Vincent, R.S. Clifton-Hadley, Parasitic infection of the seahorse (Hippocampus erectus)–a case report, J. Wildl. Dis. 25 (1989) 404–406.

[23] J.J. Campanella, L. Bitincka, J. Smalley, MatGAT: an application that generates similarity/identity matrices using protein or DNA sequences, BMC Bioinforma. 4 (2003) 29.

[24] K. Tamura, D. Peterson, N. Peterson, G. Stecher, M. Nei, S. Kumar, MEGA5: molecular evolutionary genetics analysis using maximum likelihood, evolutionary distance, and maximum parsimony methods, Mol. Biol. Evol. 28 (2011) 2731–2739.

[25] J. Prilusky, C.E. Felder, T. Zeev-Ben-Mordehai, E.H. Rydberg, O. Man, J.S. Beckmann, et al., FoldIndex: a simple tool to predict whether a given protein sequence is intrinsically unfolded, Bioinformatics 21 (2005) 3435–3438.

[26] M.M. Bradford, A rapid and sensitive method for the quantitation of microgram quantities of protein utilizing the principle of protein-dye binding, Anal. Biochem. 72 (1976) 248–254.

[27] M. De Zoysa, W.A. Pushpamali, I. Whang, S.J. Kim, J. Lee, Mitochondrial thioredoxin-2 from disk abalone (Haliotis discus discus): molecular characterization, tissue expression and DNA protection activity of its recombinant protein, Comp. Biochem. Physiol. B Biochem. Mol. Biol. 149 (2008) 630–639.

[28] D.M. Spinner, MTT growth assays in ovarian cancer, Methods Mol. Med. 39 (2001) 175–177.

[29] G.I. Godahewa, W.D. Wickramaarachchi, I. Whang, S.D. Bathige, B.S. Lim, C.Y. Choi, et al., Two carboxypeptidase counterparts from rock bream (Oplegnathus fasciatus): molecular characterization, genomic arrangement and immune responses upon pathogenic stresses, Vet. Immunol. Immunopathol. 162 (2014) 180–191.

[30] S.A. Bustin, V. Benes, J.A. Garson, J. Hellemans, J. Huggett, M. Kubista, et al., The MIQE guidelines: minimum information for publication of quantitative real-time PCR experiments, Clin. Chem. 55 (2009) 611–622.

[31] K.J. Livak, T.D. Schmittgen, Analysis of relative gene expression data using real-time quantitative PCR and the 2(-Delta Delta C(T)) Method, Methods 25 (2001) 402–408.

[32] A. Hall, P.A. Karplus, L.B. Poole, Typical 2-Cys peroxiredoxins–structures, mechanisms and functions, FEBS J. 276 (2009) 2469–2477.

[33] M. Aran, D.S. Ferrero, E. Pagano, R.A. Wolosiuk, Typical 2-Cys peroxiredoxins–modulation by covalent transformations and noncovalent interactions, FEBS J. 276 (2009) 2478–2493.

[34] B. Hofmann, H.J. Hecht, L. Flohe, Peroxiredoxins. Biol. Chem. 383 (2002) 347–364.

[35] H.J. Choi, S.W. Kang, C.H. Yang, S.G. Rhee, S.E. Ryu, Crystal structure of a novel human peroxidase enzyme at 2.0 A resolution, Nat. Struct. Biol. 5 (1998) 400–406.

[36] J. Perez-Sanchez, A. Bermejo-Nogales, J.A. Calduch-Giner, S. Kaushik, A. Sitja-Bobadilla, Molecular characterization and expression analysis of six peroxiredoxin paralogous genes in gilthead sea bream (Sparus aurata): insights from fish exposed to dietary, pathogen and confinement stressors, Fish Shellfish Immunol. 31 (2011) 294–302.

[37] G. Leyens, I. Donnay, B. Knoops, Cloning of bovine peroxiredoxins-gene expression in bovine tissues and amino acid sequence comparison with rat, mouse and primate peroxiredoxins, Comp. Biochem. Physiol. B Biochem. Mol. Biol. 136 (2003) 943–955.

[38] K. Saranya Revathy, N. Umasuthan, I. Whang, H.B. Jung, B.S. Lim, B.H. Nam, et al., A potential antioxidant enzyme belonging to the atypical 2-Cys peroxiredoxin subfamily characterized from rock bream, Oplegnathus fasciatus, Comp. Biochem. Physiol. B Biochem. Mol. Biol. 187 (2015) 1–13.

[39] M.G. Sharapov, V.I. Novoselov, V.K. Ravin, Cloning, expression and comparative analysis of peroxiredoxine 6 from different species, Mol. Biol. (Mosk) 43 (2009) 505–511.

[40] N.N. Liu, Z.S. Liu, S.Y. Lu, P. Hu, Y.S. Li, X.L. Feng, et al., Full-length cDNA cloning, molecular characterization and differential expression analysis of peroxiredoxin 6 from Ovis aries, Vet. Immunol. Immunopathol. 164 (2015) 208–219.

[41] Q. Wang, K. Chen, Q. Yao, Y. Zhao, Y. Li, H. Shen, et al., Identification and characterization of a novel 1-Cys peroxiredoxin from silkworm, Bombyx mori, Comp. Biochem. Physiol. B Biochem. Mol. Biol. 149 (2008) 176–182.

[42] Z. Hu, K.S. Lee, Y.M. Choo, H.J. Yoon, S.M. Lee, J.H. Lee, et al., Molecular cloning and characterization of 1-Cys and 2-Cys peroxiredoxins from the bumblebee Bombus ignitus, Comp. Biochem. Physiol. B Biochem. Mol. Biol. 155 (2010) 272–280.

[43] H. Wan, T. Kang, S. Zhan, H. You, F. Zhu, K.S. Lee, et al., Peroxiredoxin 5 from common cutworm (Spodoptera litura) acts as a potent antioxidant enzyme, Comp. Biochem. Physiol. B Biochem. Mol. Biol. 175 (2014) 53–61.

[44] C.A. Tairum Jr., M.A. de Oliveira, B.B. Horta, F.J. Zara, L.E. Netto, Disulfide biochemistry in 2-cys peroxiredoxin: requirement of Glu50 and Arg146 for the reduction of yeast Tsa1 by thioredoxin, J. Mol. Biol. 424 (2012) 28–41.

[45] S.N. Radyuk, V.I. Klichko, B. Spinola, R.S. Sohal, W.C. Orr, The peroxiredoxin gene family in Drosophila melanogaster, Free Radic. Biol. Med. 31 (2001) 1090–1100.

[46] G. Koopman, C.P. Reutelingsperger, G.A. Kuijten, R.M. Keehnen, S.T. Pals, M.H. van Oers, Annexin V for flow cytometric detection of phosphatidylserine expression on B cells undergoing apoptosis, Blood 84 (1994) 1415–1420.

[47] I. Banmeyer, C. Marchand, A. Clippe, B. Knoops, Human mitochondrial peroxiredoxin 5 protects from mitochondrial DNA damages induced by hydrogen peroxide, FEBS Lett. 579 (2005) 2327–2333.

[48] C. Wu, J. Gao, F. Cao, Z. Lu, L. Chen, J. Ye, Molecular cloning, characterization and mRNA expression of six peroxiredoxins from Black carp Mylopharyngodon piceus in response to lipopolysaccharide challenge or dietary carbohydrate, Fish Shellfish Immunol. 50 (2016) 210–222.

[49] C. Mu, J. Zhao, L. Wang, L. Song, H. Zhang, C. Li, et al., Molecular cloning and characterization of peroxiredoxin 6 from Chinese mitten crab Eriocheir sinensis, Fish Shellfish Immunol. 26 (2009) 821–827.

[50] W.J. Zheng, Y.H. Hu, M. Zhang, L. Sun, Analysis of the expression and antioxidative property of a peroxiredoxin 6 from Scophthalmus maximus, Fish Shellfish Immunol. 29 (2010) 305–311.

[51] B.N. Ames, M.K. Shigenaga, L.S. Gold, DNA lesions, inducible DNA repair, and cell division: three key factors in mutagenesis and carcinogenesis, Environ. Health Perspect. 101 (Suppl. 5) (1993) 35–44.

[52] L. Li, T. Kaifu, M. Obinata, T. Takai, Peroxiredoxin III-deficiency sensitizes macrophages to oxidative stress, J. Biochem. 145 (2009) 425–427.
[53] S.W. Kang, S.G. Rhee, T.S. Chang, W. Jeong, M.H. Choi, 2-Cys peroxiredoxin function in intracellular signal transduction: therapeutic implications, Trends Mol. Med. 11 (2005) 571–578.
[54] H. Park, I.Y. Ahn, H. Kim, J. Cheon, M. Kim, Analysis of ESTs and expression of two peroxiredoxins in the thermally stressed Antarctic bivalve Laternula elliptica, Fish Shellfish Immunol. 25 (2008) 550–559.
[55] P. Kling, A. Norman, P.L. Andersson, L. Norrgren, L. Forlin, Gender-specific proteomic responses in zebrafish liver following exposure to a selected mixture of brominated flame retardants, Ecotoxicol. Environ. Saf. 71 (2008) 319–327.
[56] Q. Zhang, F. Li, J. Zhang, B. Wang, H. Gao, B. Huang, et al., Molecular cloning, expression of a peroxiredoxin gene in Chinese shrimp Fenneropenaeus chinensis and the antioxidant activity of its recombinant protein, Mol. Immunol. 44 (2007) 3501–3509.
[57] L.M. Chapman, J.A. Roling, L.K. Bingham, M.R. Herald, W.S. Baldwin, Construction of a subtractive library from hexavalent chromium treated winter flounder (Pseudopleuronectes americanus) reveals alterations in non-selenium glutathione peroxidases, Aquat. Toxicol. 67 (2004) 181–194.